Theory of cyclotron resonance at a model interface in a transverse magnetic field

J.P. Vigneron and M. Ausloos
Institut de Physique, B. 5, Université de Liège, B-4000 Sart Tilman par Liège 1, Belgium
(Received 20 July 1977)

The case of a magnetic field parallel to a step junction characterizing an interface is analyzed theoretically. Comparison is made between this "transverse-field" geometry and the usual "longitudinal-field" geometry for which the applied magnetic field is perpendicular to the interface. For the transverse-field configuration, the energy eigenstates and eigenfunctions are obtained exactly. They depend on three quantum numbers: (i) p_z the particle momentum parallel to the field, (ii) p_y measuring the distance between the center of the charge-carrier oscillation and the interface, and (iii) n the Landau-level label. Different regimes are examined as a function of the step potential height with special emphasis on the case where the center of oscillation is on the interface ($p_y = 0$). For this case, selection rules for magneto-optical absorption predict strong harmonics especially for high potential steps. Reference is made to rare experimental data. The energy levels and wave functions of an electron in a uniform magnetic field can also be obtained by means of a transfer-matrix technique for an arbitrary set of step potentials.

I. INTRODUCTION

During the last decades an increasing amount of work has been invested in the study of physical systems such as semiconductor or metal surfaces, p-n semiconductor junctions and related topologies. Due to their complexity, the system properties have to be described in terms of approximate models. The usual approach starts with a choice between either solving approximately an involved model containing much of the details of the real system or solving exactly a simplified model containing its qualitative features only. In the present paper, the latter approach will be considered for studying the effects of a magnetic field on energy states at an interface, and for considering the possibility of their detection by cyclotron-resonance experiments.

Applied magnetic fields are standard experimental constraints[1] used to investigate the Fermi surface of metals and the bottom (top) of the conduction (valence) band in semiconductors. Parameters such as band masses and the nonparabolicity of the band have been often studied using the data provided by cyclotron-resonance experiments.

After such successful application in semiconductors and metals, one conjectures that this powerful technique (i.e., magnetic quantization) can be used to study other systems, such as surfaces or junctions.[2,3] Few examples of such experiments have been reported so far.[2-12] In most cases, the magnetic field has been directed along the direction of the potential gradient ("longitudinal field"), i.e., perpendicular to the interface.[4-8] A few experiments[9-12] with the field parallel to the interface have been reported. For the former configuration, the electron interacts with the potential step only through the translational part of its helicoidal motion along the magnetic field, except when the presence of the interface induces variations in the transverse (parallel to the surface) potential. This is the case, for instance, when the interface considered presents some irregularities or when a band bending occurs. Several papers by Ando have appeared on this subject.[13] The case of surface roughness will be discussed by us elsewhere.[14]

It appears from such works that the cyclotron resonance variation in the *longitudinal-field* geometry does not seem to be directly connected to the height of the potential step but rather to the number and distribution of the traps lying near the interface and to the gradient of potential perpendicular to the interface.[14] On the other hand, another range of information can be provided by the *transverse-field* configuration. In this case, where the magnetic field is parallel to the interface, hence perpendicular to the potential gradient, it is easy to visualize that the orbiting electron now strongly and directly interacts with the potential jump.

In a first approximation, one can consider the interface potential variation to be described by a step discontinuity. For example, at a semiconductor or metallic surface, this discontinuity can represent the energy difference between the vacuum and the Fermi level inside the material. Similarly, such a discontinuity corresponds to the energy difference between the energy levels in the p and n regions at an appreciable distance of the junction. It is known that such a junction can be better described in terms of an asymmetric barrier potential (Fig. 1), the height and width of which can, in principle, be adjusted by doping.

Here, therefore, we treat the limiting case of

a heterojunction where the only energy discontinuity arises from conduction band discontinuity. Models with other profiles can often be qualitatively discussed along the lines of our calculation by using appropriate values for their heterojunction characteristics.

We realize nevertheless the limitation of our model, as an interface description. Furthermore we neglect all scattering mechanisms, and do not consider limitations due to finite-penetration depth. Scattering mechanisms associated with the interface itself could introduce some non-negligible damping and relaxation indeed. In particular, they could play an important role in reducing the sharpness of the cyclotron resonance main peak and harmonics which we calculate in the following sections. However, even with an elementary model such as a step barrier, the following theoretical investigation can already shed some light on data interpretation for a real experiment.

The rather academic step potential model can be rightly modified to be much more appropriate physically, and much more useful, in describing the thin repeated heterostructure fabricated by molecular-beam epitaxy.[15] The one-dimensional regular Kronig-Penney model in a magnetic field is quite appropriate here, beside being an interesting exercise in elementary quantum mechanics. The results can only be numerical, and can be easily obtained by some skilled calculator. More realistic and complicated physical conditions (e.g., random Kronig-Penney model in a magnetic field) can also be calculated later.

The magnetic-field-step-discontinuity model solved in the present paper describes the system as an isolated particle moving in a one-dimensional step potential placed in a uniform magnetic field. The following calculation is equivalent to solving exactly the one-dimensional harmonic oscillator problem with a step discontinuity. This model is given in more detail in Sec. II, where the exact eigenstates and eigenvalues are obtained and discussed for particular cases. In Appendix A, a perturbation treatment for a shallow discontinuity is given. In Sec. III, exact results are obtained for the optical absorption of the model described in Sec. II. The Transfer matrix method in a uniform field is treated in Appendix B. A brief discussion can be found in Sec. IV.

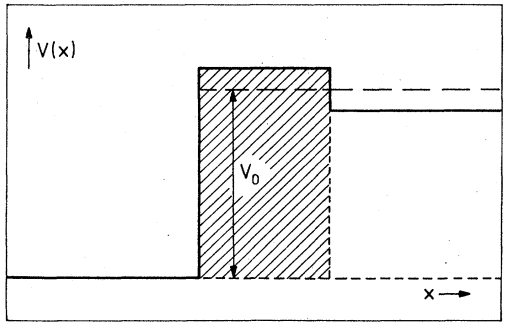

FIG. 1. p-n junction with doped interface region (shadowed region) considered as a single-step discontinuity.

II. EXACT SOLUTION

Let the potential be a constant V_0 (zero) on the right (left) of the plane $x=0$, and B be the magnitude of a uniform constant magnetic field applied along the z direction (Fig. 2).

Such a geometry where B is perpendicular to the direction of the "potential gradient" is for the purpose of this work the most interesting one since it allows the particle orbit to cross the plane of potential discontinuity. Hence this particle is a good system for testing the characteristics of both regions.

In the Landau gauge, the vector potential is chosen to be $\vec{A}=B(0,x,0)$. The Hamiltonian of a particle in the total potential is then given by

$$H = \frac{p_x^2}{2m} + \frac{[p_y - (eB/c)x]^2}{2m} + \frac{p_z^2}{2m} + V_0\Theta(x), \qquad (1)$$

where $\Theta(x)$ is the Heaviside step function.

After performing a unitary transformation of the Hamiltonian $S^{-1}HS$, with $S=\exp[-i(cp_y/eB)p_x]$, the new Hamiltonian is the sum of three terms: (i) a harmonic-oscillator Hamiltonian along the x axis, (ii) a free-particle kinetic energy along the z axis, and (iii) a shifted step potential at the point $x_0=-cp_y/eB$.

In making this transformation x_0 becomes simply the distance between the step and the center of the classical orbit described by the particle in the constant magnetic field. This distance is a constant of the motion.

At this point, it is more convenient to use re-

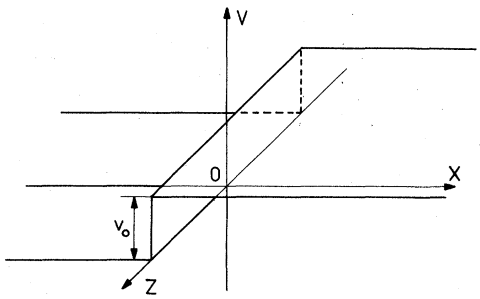

FIG. 2. Geometry of the problem: a step discontinuity v_0 in the potential energy of the particle takes place on the plane $x=0$. A uniform magnetic field B is applied in a plane perpendicular to the x axis and defines the z axis.

duced units, where (a) lengths are expressed in units of the cyclotron radius $r_0=(\hbar/2m\omega_c)^{1/2}$; (b) masses in units of $2m$; (c) time is written in units of ω_c^{-1}, where m and ω_c are the particle mass and cyclotron frequency eB/mc, respectively. In such units, energy, and momentum are expressed in units of $\hbar\omega_c$ and $(2m\hbar\omega_c)^{1/2}$.

Since $[p_y, H]=[p_z, H]=0$, the wave function $\Psi(\vec{r})$ can readily be written as the product of plane waves along y and z direction times a function $w(x)$ which satisfies the following equation:

$$[p_x^2+\tfrac{1}{4}x^2+U(x)]w(x)=\epsilon w(x), \tag{2}$$

where ϵ is related to the total energy E of the particle by $\epsilon=E-p_z^2$ and $U(x)=v_0\Theta(x+2p_y)$. The potential is drawn in Fig. 3. The Schrödinger equation (2) is solvable independently in regions I and II joining at $x=-2p_y$.

In each region, this equation has two linearly independent solutions the so-called parabolic cylinder functions.[16] In region I ($x<-2p_y$) and region II ($x>-2p_y$), the solutions are, respectively,

$$w_{\mathrm{I}}=AU(-\epsilon,x)+BV(-\epsilon,x), \tag{3a}$$

$$w_{\mathrm{II}}=CU(-\epsilon+v_0,x)+DV(-\epsilon+v_0,x). \tag{3b}$$

However, all values of A, B, C, D are not allowed. They have to be such that $w(x)$ is a square integrable function. Considering the asymptotic behavior of the parabolic cylinder functions Eqs. (19.4.2) and (19.4.3) of Ref. 16 one must keep only the following expressions:

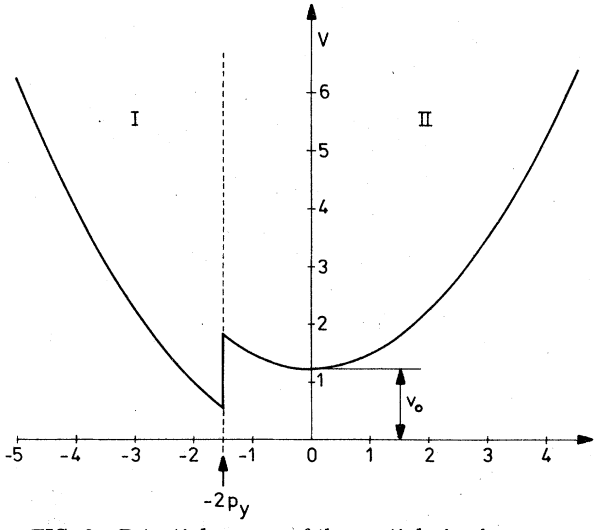

FIG. 3. Potential energy of the particle is shown as a function of the distance of the center of the classical orbit with respect to the step junction. The plane $x=-2p_y$ separates the space into regions I and II in which harmonic oscillator potentials differ by a constant v_0. Reduced units are used.

$$w_{\mathrm{I}}=[B\Gamma(\tfrac{1}{2}-\epsilon)/\pi]\,U(-\epsilon,-x), \tag{4a}$$

$$w_{\mathrm{II}}=CU(-\epsilon+v_0,x), \tag{4b}$$

which obey the requirement $w_{\mathrm{I}}(x\to-\infty)=0$ and $w_{\mathrm{II}}(x\to\infty)=0$.

The usual matching conditions at $-2p_y$ lead to an homogeneous system of equations which produces nontrivial solutions only if the following requirement is satisfied:

$$U(-\epsilon-1,2p_y)U(-\epsilon+v_0,-2p_y)+U(-\epsilon,2p_y)U(-\epsilon-1+v_0,-2p_y)=0. \tag{5}$$

This equation implicitly defines the eigenvalues of the Hamiltonian. It is then possible to write a closed form for the normalized wave function corresponding to the eigenvalue $\epsilon(v_0,p_y)$, i.e.,

$$w_{\mathrm{I}}=C[U(-\epsilon+v_0,-2p_y)/U(-\epsilon,2p_y)]\,U(-\epsilon,-x), \tag{6a}$$

$$w_{\mathrm{II}}=CU(-\epsilon+v_0,x), \tag{6b}$$

where

$$C^{-2}=\int_{-2p_y}^{\infty}U^2(-\epsilon+v_0,x)\,dx+\frac{U^2(-\epsilon+v_0,-2p_y)}{U^2(-\epsilon,2p_y)}\int_{2p_y}^{\infty}U^2(-\epsilon,x)\,dx. \tag{7}$$

There is, in principle, no difficulty in solving (5) numerically or analytically for some values of v_0 and p_y. Therefore, expression (6) can be evaluated exactly. However to obtain the normalization C^{-2} is more difficult because there is no general expression known for the integrals appearing in Eq. (7) except in a few special cases.

One of these cases arises when the orbit center is pinned on the position of the step discontinuity of the potential ($p_y=0$). Another completely solvable situation corresponds to the case of very high step potential ($v_0\to\infty$). The complete resolution of these cases with respect to the energies and the wave functions is illustrative of the way the solutions behave in the general case.

The case $p_y=0$ is an interesting nontrivial case for which the general form of parabolic cylinder functions are not explicitly needed. Equation (5) can be rewritten in terms of Γ functions

$$\frac{1}{\Gamma(\frac{1}{4}-\frac{1}{2}\epsilon)}\,\frac{1}{\Gamma(\frac{3}{4}-\frac{1}{2}\epsilon+\frac{1}{2}v_0)}+\frac{1}{\Gamma(\frac{3}{4}-\frac{1}{2}\epsilon)}\,\frac{1}{\Gamma(\frac{1}{4}-\frac{1}{2}\epsilon+\frac{1}{2}v_0)}=0. \tag{8}$$

The energies ϵ can be evaluated from this equation as a function of the potential step strength v_0. The results are displayed in Fig. 4.

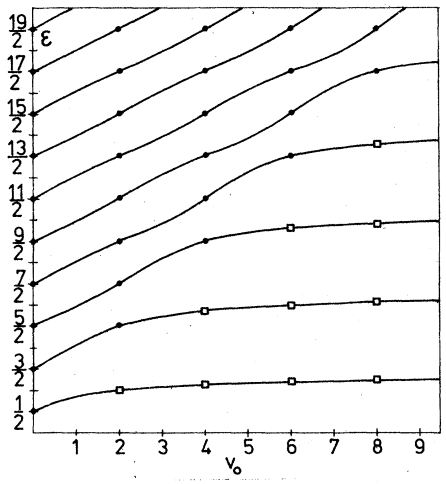

FIG. 4. Energy diagram versus the step amplitude v_0 for $p_y=0$. The levels move from $n+\frac{1}{2}$ to $(2n+1)+\frac{1}{2}$ in units of $\hbar\omega_c$ as v_0 increases from zero to infinity.

Furthermore, a few special energy states can be exactly obtained. First define

$$a=\tfrac{1}{4}-\tfrac{1}{2}\epsilon\ . \tag{9}$$

When $v_0=2n$ (even integer), Eq. (20) has the simple form

$$[(a)_n+(a+\tfrac{1}{2})_n]/\Gamma(a+n)\Gamma(a+\tfrac{1}{2}+n)=0\,, \tag{10}$$

where $(a)_n$ is the Pochhammer symbol defined equivalently by[16]

$$(a)_n=a(a+1)(a+2)\cdots(a+n-1)\ . \tag{11}$$

The poles of $\Gamma(a+n)$ and $\Gamma(a+n+\frac{1}{2})$ are immediate solutions of (10), which lead to the energy levels shown by *black dots* in Fig. 4. On the other hand,

$$(a)_n+(a+\tfrac{1}{2})_n=0 \tag{12}$$

is an algebraic equation of degree n. The roots calculated from (12) are indicated by *squares* in Fig. 4.

Starting from the general expression for the wave function, Eq. (6), with $p_y=0$, one has

$$w_{\rm I}(x)=C\,\frac{2^{-v_0/2}\Gamma(\frac{3}{4}-\frac{1}{2}\epsilon)}{\Gamma(\frac{3}{4}-\frac{1}{2}\epsilon+\frac{1}{2}v_0)}\,U(-\epsilon,-x)\,, \tag{13a}$$

$$w_{\rm II}(x)=CU(-\epsilon+v_0,x)\,, \tag{13b}$$

with C^{-2} expressed as[17]

$$C^{-2}=2^{-3/2}\sqrt{\pi}\left[A(-\epsilon+v_0)+\left(\frac{\Gamma(\frac{3}{4}-\frac{1}{2}\epsilon)}{\Gamma(\frac{3}{4}-\frac{1}{2}\epsilon+\frac{1}{2}v_0)}\right)^2 2^{-v_0}A(-\epsilon)\right], \tag{14}$$

with $A(x)$ given by

$$A(x)=[\Psi(\tfrac{1}{2}x+\tfrac{3}{4})-\Psi(\tfrac{1}{2}x+\tfrac{1}{4})]/\Gamma(x+\tfrac{1}{2})\,. \tag{15}$$

In this expression, $\Psi(x)$ is the logarithmic derivative of $\Gamma(x)$.

To illustrate the behavior of the wave functions, a few are shown in Figs. 5 and 6 for the ground state and the first excited state, respectively. The wave functions are calculated for $v_0=0$ (harmonic-oscillator problem), $v_0=1$ or 2, and $v_0=\infty$ (half-harmonic-oscillator well). It can be seen that the wave function shifts toward the center of the left well when v_0 increases. Its shape changes from the wave function of the harmonic oscillator $n+\frac{1}{2}$ state for $v_0=0$ into the x-negative wave function of the harmonic-oscillator $(2n+1)+\frac{1}{2}$ state for $v_0=\infty$. For such a condition, the wave function vanishes identically for x positive. In this latter case, half of the harmonic oscillator levels "survive," and are those corresponding to odd parity states.

For intermediate values of v_0, the wave function arises from a mixture of states. In particular, when v_0 is an even integer, (see above) it can be easily shown that the wave functions fall in two categories: one for which the corresponding energy ϵ is greater than v_0; the other for which ϵ is smaller than v_0.

In the first case, if $\epsilon=l+\frac{1}{2}$ with $l=v_0, v_0+1, v_0+2,\ldots$, the wave function in the left-hand side well (x negative) is that of the $l+\frac{1}{2}$ harmonic-oscillator state and matches that of the $l-v_0+\frac{1}{2}$ harmonic-oscillatr state at $x=0$. In the right-hand side well (x positive), the wave function is that of the $l-v_0+\frac{1}{2}$ harmonic-oscillator state.

The second category of wave functions does not allow such a simple description, because in the left-hand side well, energy states are not exactly that of a harmonic oscillator. They belong to the saturated part of the energy curves versus v_0 (see Fig. 4). In the right-hand side well, wave functions are naturally damped.

The next interesting special case is that of an infinitely large step height v_0 for an arbitrary orbit center.

In this limit, the eigenfunctions are

$$w_{\rm I}(x)\sim U(-\epsilon(p_y),-x);\quad w_{\rm II}(x)=0\ . \tag{16}$$

The matching condition is readily found to be

$$w_{\rm I}(-2p_y)=0\,. \tag{17}$$

The roots of $U(-\epsilon,+2p_y)$ remain to be found. Some (marked by a *black dot* in Fig. 7) are those of Hermite polynomials. On the other hand, the asymptotic behavior of $U(a,x)$ for $x\to-\infty$ implies that the values of a for which $U(a,x)$ vanishes in that limit approach $n-\frac{1}{2}$. Such an asymptotic behavior is easily seen on Fig. 7 and admits of a simple

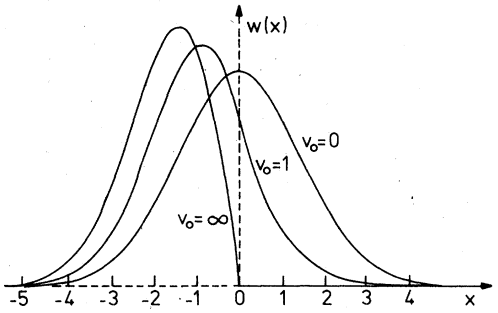

FIG. 5. Evolution of the ground state wave function $w(x)$ as v_0 increases from zero to infinity, in the case $p_y=0$. The $n=0$ oscillator state for $v_0=0$ moves toward the $n=1$ oscillator state (defined only for $x<0$ when v_0 tends to infinity).

interpretation in terms of the step discontinuity motion toward the left ($p_y \to \infty$) or the right ($p_y \to -\infty$). The motion of the oscillation center and the energy level position are interpreted similarly: when p_y is very large, the potential well is narrow and high with respect to the harmonic-oscillator ground state and hence, energy levels have a high value.

When p_y decreases ($p_y \sim 0$ and further $\to -\infty$) the potential well looks more and more similar to that of a harmonic oscillator, thereby explaining the asymptotic value of $\epsilon(p_y)$.

Possible extensions of our work are suggested. It would be interesting to consider (i) different band masses on each side of the interface; (ii) an asymmetrical step barrier (thus with three different band masses), better characterizing usual junctions. Extensions toward tunneling experiments would follow (iii) the regular Kronig-Penney model in a magnetic field; (iv) the infinite linear chain disordered Kronig-Penney model in a magnetic field; and (v) the finite chain

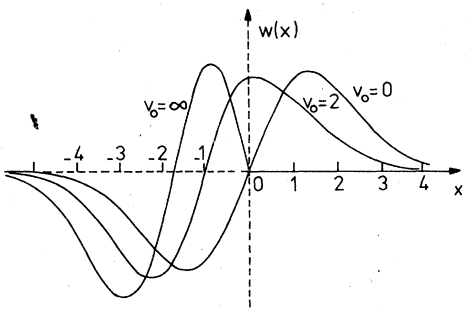

FIG. 6. Evolution of the first excited state for v_0 varying from zero to infinity for $p_y=0$. The wave function for $v_0=2$, e.g., is built from the $n=0$ oscillator state for x positive matched to the $n=2$ oscillator state for negative abscissas.

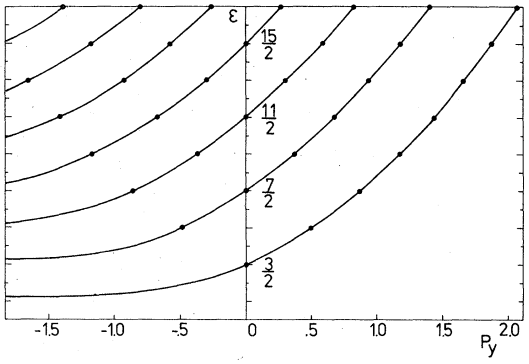

FIG. 7. Dispersion relation $\epsilon(p_y)$ in the limiting case $v_0 \to \infty$. The black dots correspond to energies $\epsilon = n + \frac{1}{2}$ and are given by $X_{\mu,n}/\sqrt{2}$ where $X_{\mu,n}$ ($\mu = 1, 2, \ldots, n$) are the zeros of the n-degree Hermite polynomial. The saturation obtained for $p_y \to -\infty$ corresponds to simple Landau levels when the center of the classical orbit is far from the step discontinuity.

for models (iii) and (iv).

In order to solve these problems, the transfer-matrix technique is the most appropriate. This is only an extension of the present work. The general procedure is established in Appendix B.

III. OPTICAL TRANSITIONS

In the preceding sections the exact eigenstates and corresponding energies have been derived. From these, the physical properties of the system can be easily obtained. As an example one may examine features of the optical process in such a system.

The absorption spectrum of a system with a step potential is the superposition of[1] an absorption taking place far inside the solid, in the low-potential region,[2] an absorption of light by the particles orbiting near the step, and[3] an absorption by particles moving in the high-potential region. These cases correspond, in our formalism, to the conditions $p_y \ll 0$, $p_y \approx 0$, $p_y \gg 0$, respectively. More generally, knowing the absorption coefficient for a fixed value of p_y, one can deduce the whole absorption spectrum arising from the spatial distribution of the orbit centers by a mere convolution. Only $p_y=0$ will be explicitly treated here because of its experimental interest. At the end of the section some argument will be given in order to predict the distortion due to a given distribution of orbit centers.

As can easily be understood, the absorption due to particles in the high-potential region is small, since, at the low temperatures required to obtain sharp cyclotron lines, these states are not populated. This is strongly justified in real systems, where the magnetic energy $\hbar\omega_c$ is generally

small compared to the step amplitude for practically accessible magnetic field strengths and actual values of effective masses.

For these conditions, the only cases which remain to be considered are these corresponding to $p_y \ll 0$ and $p_y \approx 0$. The former is nothing more than the "bulk" contribution which has been extensively studied in many semiconductors.

This would lead to a strong absorption peak at $\omega = \omega_c$ if an active mode of the incident radiation is selected. To illustrate the specific absorption arising from the interaction of the orbiting electron with the potential wall, let us thus consider the case $p_y = 0$.

At zero temperature and relatively weak incident intensities the Fermi Golden Rule allows one to calculate the absorption coefficient $\Gamma(\omega)$. Considering that all transitions start from the ground state ($p_z = 0$; $n = 0$), one writes

$$\Gamma(\omega) = \frac{16\pi^2 \alpha_r n_e}{n\omega} \times \sum_{n, p_z'} |\langle n, p_z' | \vec{\pi} \cdot \vec{\eta} | 0, 0 \rangle|^2 \, \delta(\epsilon_f - \epsilon_i - \omega), \tag{18}$$

where ϵ_f and ϵ_i are, respectively, the final and initial energy levels. Reduced units are used and, in particular, the absorption coefficient is given here in units of the inverse cyclotron radius r_0^{-1}; α_r is the fine-structure constant; n_e is the carrier concentration near the interface; and n is the refractive index in the material.

In the case where the linear polarization is directed along the magnetic field axis, the matrix element $\langle f | p_z | i \rangle$ identically vanishes as soon as the initial state is the state $p_z = 0$. No cyclotron absorption is thus expected in the configuration where the electric component of the radiation is parallel to the steady magnetic field. This is identical to the case of the "bulk" absorption.

The complete expression (18) can be computed to obtain the relative peak strengths. They are displayed in Fig. 8 for several values of v_0 at the calculated positions of the absorption frequency in the case where the polarization is perpendicular to the interface. One clearly sees the rapid increase of higher-order harmonics as v_0 increases. The order of the dominant harmonics apparently depends on the value of v_0 in a rather complicated way. Neverthelss, inspection of Fig. 8 indicates that all important harmonics always lie in regions near the frequencies $(2n + 1/2)\hbar\omega_c$, which represent the saturation energies pointed out in Sec. II.

This remark is more convincing when the $v_0 \gg 1$ spectra are considered; it is less evident

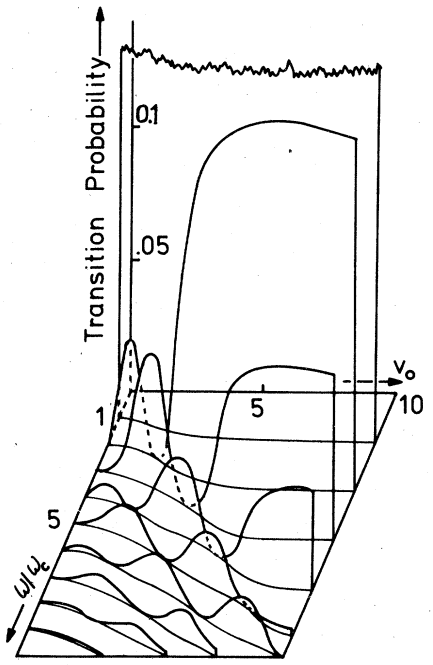

FIG. 8. Position and relative strengths of the absorption peaks arising from allowed transitions at fixed field for various values of the step amplitude v_0. It can be seen that the number of harmonics increases when v_0 increases.

for $v_0 < 1$, where harmonics have a rather small strength. Nevertheless, this information, added to the fact that the strength of the shifted cyclotron resonance peak is always very strong is important for the data analysis and interpretation of the very structured spectrum predicted in the configuration studied here.

The limitation for effectively observing these transitions is twofold: first, condition $p_y = 0$ will never be strictly achieved. Some distribution of p_y values around $p_y = 0$ is unavoidable because the carrier orbit centers fluctuate near the interface even though some strong driving force is imposed in order to concentrate the carriers on the interface.

This induces some line broadening provided that the energy levels are p_y dependent, due to the variation of the potential.

However, it may be pointed out that, for high-potential steps, energy separations can be seen to be almost always larger than $\hbar\omega_c$ (see Fig. 4). No important contribution to the absorption is thus expected for $\hbar\omega < \hbar\omega_c$ even in the case of a broad distribution of orbit centers. The absorption line will then be distorted, and will mainly broaden toward high frequencies. The main line is thus expected to be more or less asymmetrical depending on the

actual orbit-center distribution.

Furthermore, all kinds of scattering processes (involving impurities, phonons, etc.) are responsible for a broadening of the lines. The experimental arrangement should then take into account these effects: (a) by localizing as much as possible the orbits near the interface (for instance by applying an electric field in y direction); and (b) by searching for optimal conditions (low temperature, high purity of the sample, good definition of the interface).

On the other hand, one can suggest that the polarization direction of the incident radiation be varied. It is easy to show that although the matrix elements $\langle f | p_x | i \rangle$ and $\langle f | -\frac{1}{2} x | i \rangle$ are equal in the limit $v_0 = 0$, this will generally not be true in the case $v_0 \neq 0$. The change recorded in the spectrum going from $\vec{\eta} = (1, 0, 0)$ to $(0, 1, 0)$ is specifically due only to the presence of the step potential.

Furthermore, if one considers the nonactive circular polarization $\vec{\eta} = (1, -i, 0)/\sqrt{2}$, no line is expected in the spectrum when $v_0 = 0$ (i.e., in the bulk). For $v_0 \neq 0$ therefore, any observed structure should be due only to absorptions by carrier orbiting near the interface. For such an experimental configuration, the spectrum is thus highly sensitive to the presence of a potential gradient.

IV. CONCLUSION

In this paper, the behavior of a particle moving in a uniform magnetic field and orbiting near a potential step discontinuity is examined theoretically. The magnetic field is set up parallel to the direction of the strong one-dimensional potential gradient in contrast to the configuration generally used so far in interface probing experiments.

The problem can be treated easily: some results are analytically obtained, other need some graphical or numerical processing.

It is shown that the eigenstates for such a system are described by three quantum numbers: p_z, which characterizes the particle momentum in the magnetic field; p_y, which here is related to the distance between the center of the classical orbit and the step discontinuity; and n, which takes positive integer values and characterizes the generalized Landau level (p_y and p_z fixed). In the framework of this model, optical abosrption selection rules and strength are predicted and discussed.

The transverse configuration which is studied here can be considered as complementary to the usual longitudinal-field configuration. It seems, however, that this transverse configuration is more sensitive to the value of the potential height, while the former is a better test of the surface structure and roughness.

In both cases, one has to take into account the distribution (or the density) of oscillation centers, if the predicted fine structure of the resonance lines has to be analyzed. This distribution is unavailable at this time. Hence we have considered a relevant case for which the oscillation centers are close to the interface.

Some emphasis has indeed been put on the case $p_y = 0$. One might ask whether it is possible to localize the orbit centers on the discontinuity. Such a stiuation could be obtained by applying a weak electric field *parallel* to the interface, but *perpendicular* to the magnetic field. In this case, it is possible to drive the oscillation centers towards the interface, where the density of carriers with $p_y = 0$ would then become larger.

Even for very large applied magnetic fields (say 100 kOe) the bulk cyclotron resonance frequency ω_c is usually quite small (i.e., in the meV range). In typical cases V_0 varies from $\frac{1}{2}$ to 6 eV. Hence the dimensionless parameter v_0 ranges from 10^2 to 10^3. Such a value of v_0 can however be reduced if the effective mass of the carrier is small.

In this respect, thin-layered semiconducting heterostructures are probably the most interesting cases where the results of the present paper should apply. In these materials, much smaller jumps of potential can be created. The situation where $v_0 \approx \hbar \omega_c$ can be found much more easily and the whole transition range $1 < v_0 < 10$ can then be studied. However, one must keep in mind that *larger* v_0 values are not of negligible interest and belong in fact to another range of physical situations. They correspond in this work to the *saturation regime* in which "half" the Landau levels exist. Various strong harmonics are in fact predicted in absence of damping effects.

An interesting case of the use of the transverse-field geometry to investigate an interface has been provided by the Beinvogl, Kamgar, and Koch experiment[10] on Si(100) surface. For typical magnetic fields this case is an example of a very high step ($v_0 = \infty$). However, the band bending is here too large to allow the use of the simple-step model. Indeed, the potential depth (or band bending) at the surface is of the order of 50 meV,[13] while, even for the large applied magnetic field (i.e., 10 T), $\hbar \omega_c$ is of the order of 5 meV only. The band bending cannot be considered as a perturbation. An extension of the step problem to allow piecewise linear potentials should be much more appropriate to treat the available data in the transverse field configuration. Such a problem can

be later handled by a transfer matrix technique similar to that described in Appendix B.

APPENDIX A

Here the perturbation method is applied to the calculation of eigenvalues and eigenfunctions in the limiting case of a small-step amplitude v_0.

The unperturbed Hamiltonian is written

$$H_0 = a^\dagger a + \tfrac{1}{2}, \tag{A1}$$

where the operators a and $a^\dagger$, defined by $a = \frac{1}{2}x + ip_x$, and $a^\dagger = x/2 - ip_x$, obey the usual boson commutation relation.[18]

Using the Fourier transform of the Heaviside step function, the perturbation potential can be expressed as

$$V = \lim_{\eta \to 0+} \left(-\frac{v_0}{2i\pi}\right) \times \int_{-\infty}^{+\infty} \frac{e^{-\omega^2/2} e^{-i\omega a^\dagger} e^{-i\omega a} e^{-2i\omega p_y}}{\omega + i\eta} \, d\omega \, . \tag{A2}$$

It is then simple to obtain the first-order correction to the ground-state energy under the form

$$\Delta\epsilon^{(1)} = -\lim_{\eta \to 0+} \frac{v_0}{2i\pi} \int_{-\infty}^{+\infty} \frac{e^{-\omega^2/2} e^{-2i\omega p_y}}{\omega + i\eta} \, d\omega \, , \tag{A3}$$

which reduces to

$$\Delta\epsilon^{(1)} = (\tfrac{1}{2} v_0)[1 - \mathrm{erf}(-\sqrt{2}\, p_y)] \, . \tag{A4}$$

In the second-order correction $\Delta\epsilon^{(2)}$, the matrix element $\langle 0 \,|\, V \,|\, n \rangle$ needs to be calculated

$$\langle 0 \,|\, V \,|\, n \rangle = \frac{v_0}{2\pi} \frac{(-i)^{n-1}}{\sqrt{n!}} \times \int_{-\infty}^{+\infty} \frac{\omega^n}{\omega + i\eta} \, e^{-2i\omega p_y} e^{-\omega^2/2} \, d\omega \, . \tag{A5}$$

Cases with n odd or even have to be calculated separately using relations (3.952.9) and (3.952.10) in Ref. 16. Both lead to a concise expression

$$\langle 0 \,|\, V \,|\, n \rangle = [v_0/(\pi n! \, 2^n)^{1/2}] \exp(-2p_y^2) H_{n-1}(-\sqrt{2}\, p_y) \, , \tag{A6}$$

where $H_n(x)$ is the Hermite polynomial of degree n, from which the factor $|\langle 0 \,|\, V \,|\, n \rangle|^2$ can be calculated and inserted into standard expressions for $\Delta\epsilon^{(2)}$. Correspondingly, $\langle 0 \,|\, V \,|\, n \rangle$ serves to evaluate the first-order correction to the wave function.

Excited states can be calculated straightforwardly, but with some more algebra, starting from the matrix elements

$$\langle n \,|\, V \,|\, m \rangle = \frac{v_0}{2} \left(\frac{[n(n-1)\cdots(m+1)]^{1/2}}{(n-m)!} F_{n-m}(-2p_y) + \sum_{j=1}^{m} \frac{[n(n-1)\cdots j]^{1/2} [m(m-1)\cdots j]^{1/2}}{(n-j+1)!\,(m-j+1)!} F_{n+m-2j+2}(-2p_y) \right) \tag{A7}$$

for $n > m$, with

$$F_m(x) = (2^{1-m/2}/\sqrt{\pi}) e^{-x^2/2} H_{m-1}(x/\sqrt{2}) \, . \tag{A8}$$

The case $n < m$ is readily expressed from the above, while the diagonal element is

$$\langle n \,|\, V \,|\, n \rangle = \frac{v_0}{2} \left[F_0(-2p_y) + \sum_{k=1}^{n} \frac{n!}{(n-k)!} \times \left(\frac{1}{k!}\right)^2 F_{2k}(-2p_y) \right] , \tag{A9}$$

where

$$F_0(x) = \mathrm{erfc}(x/\sqrt{2}) \, . \tag{A10}$$

Furthermore, from these matrix elements the first-order correction to the excited-state wave function can be readily obtained, starting from standard formulas.

APPENDIX B

Here we present the expressions required for treating more-realistic cases than the single-step potential by means of a transfer-matrix technique. This formulation allows one to handle problems presenting several potential jumps, and this encompasses a very wide range of physical situations.[2,15]

Let us suppose a distribution of a finite number of potential steps at the points x_l, $l = 1, \ldots, N$. The potential $U(x)$ in region l, i.e., between x_{l-1} and x_l is v_l. In this region, the wave function can be written

$$w_l(x) = A_l \, U(v_l - \epsilon, x) + B_l \, V(v_l - \epsilon, x) \, . \tag{B1}$$

All these wave functions must be matched at each point $x_l - 2p_y$. This imposes a linear relation between coefficients in region l and $l+1$. This relation can be put into a matrix form

$$\begin{pmatrix} A_l \\ B_l \end{pmatrix} = T^{(l)} \begin{pmatrix} A_{l+1} \\ B_{l+1} \end{pmatrix}, \tag{B2}$$

where

$$T^{(l)} = t^{-1}(v_l, x_l)\, t(v_{l+1}, w_l) \tag{B3}$$

and

$$t(v_l, x_l) = \begin{pmatrix} U(v_l - \epsilon, x_l - 2p_y) & V(v_l - \epsilon, x_l - 2p_y) \\ U'(v_l - \epsilon, x_l - 2p_y) & V'(v_l - \epsilon, x_l - 2p_y) \end{pmatrix}. \tag{B4}$$

Note that the Wronskian of U and V, i.e., $\det t(v_l, x_l)$, is equal to $(2/\pi)^{1/2}$. It is then very simple to invert $t(v_l, x_l)$ to obtain the complete transfer matrix $[T_{ij}^{(l)}] = (\frac{1}{2}\pi)^{1/2}[\mathcal{T}_{ij}^{(l)}]$ which has elements

$$\begin{aligned}
\mathcal{T}_{11}^{(l)} &= V(v_l - \epsilon + 1, X_l)U(v_{l+1} - \epsilon, X_l) \\
&\quad + (v_{l+1} - \epsilon + \tfrac{1}{2})U(v_{l+1} - \epsilon + 1, X_l)V(v_l - \epsilon, X_l), \\
\mathcal{T}_{12}^{(l)} &= V(v_l - \epsilon + 1, X_l)V(v_{l+1} - \epsilon, X_l) \\
&\quad - V(v_{l+1} - \epsilon + 1, X_l)V(v_l - \epsilon, X_l), \\
\mathcal{T}_{21}^{(l)} &= (v_l - \epsilon + \tfrac{1}{2})U(v_l - \epsilon + 1, X_l)U(v_{l+1} - \epsilon, X_l) \\
&\quad - (v_{l+1} - \epsilon + \tfrac{1}{2})U(v_{l+1} - \epsilon + 1, X_l)U(v_l - \epsilon, X_l), \\
\mathcal{T}_{22}^{(l)} &= V(v_{l+1} - \epsilon + 1, X_l)U(v_l - \epsilon, X_l) \\
&\quad + (v_l - \epsilon + \tfrac{1}{2})U(v_l - \epsilon + 1, X_l)V(v_{l+1} - \epsilon, X_l),
\end{aligned} \tag{B5}$$

where the first index labels lines of the matrix and $X_l = x_l - 2p_y$.

There is an essential difference between the present situation and that in the absence of a magnetic field. Because of the existence of a center of oscillation when a field is applied, the wave function is localized around this center and thus has to be square integrable here along the potential gradient direction. For a given value of p_y (that is, for a given position of the oscillation center), the spectrum of eigenvalues is discrete. In the absence of a magnetic field, the spectrum is continuous and the solutions are described in terms of nonsquare integrable plane waves.

Here, for $x > x_N$ and $x < x_1$, the potential is supposed to be zero thereby implying that the solutions have to vanish when $|x| \to \infty$. This imposes $B_{N+1} = 0$ on one hand, and

$$\prod_{l=N}^{1} T^{(l)} \begin{pmatrix} 1 \\ 0 \end{pmatrix} = \alpha \begin{pmatrix} \sin\pi\epsilon \\ \pi/\Gamma(\frac{1}{2} - \epsilon) \end{pmatrix} \tag{B6}$$

on the other hand, where α is some constant. This last condition arises from the fact that

$$U(-\epsilon, -x) = \sin(\pi\epsilon)U(-\epsilon, x) + [\pi/\Gamma(\tfrac{1}{2} - \epsilon)]\, V(-\epsilon, x) \tag{B7}$$

is the *only* combination of $U(-\epsilon, x)$ and $V(-\epsilon, x)$ that vanishes for $x \to -\infty$. Relation (B6) can be transformed into the more easily tractable equation

$$\left(\frac{-\pi}{\Gamma(\frac{1}{2} - \epsilon)}, \sin\pi\epsilon \right) \prod_{l=N}^{1} T^{(l)} \begin{pmatrix} 1 \\ 0 \end{pmatrix} = 0. \tag{B8}$$

Such a requirement allows one to obtain exact energies and wave functions for a given position of the orbit center.

In principle, this method can be applied to a large number of potential steps, whereas the only limitation lies in the precision required in computing parabolic cylinder functions. Hence, it is reasonable to believe that the transfer matrix method and Eq. (B8) should provide an interesting way of solving exactly a (random or regular) Kronig-Penney model in a magnetic field. In this case, it seems, however, that due to the localization of the wave function around the orbit center, at least for lower energies, only a finite number of cells need to be considered. This is precisely the case where the above technique could be successfully applied.

An attempt to solve the Kronig-Penney model in a magnetic field has recently been provided by Taylor.[19] In this calculation, a matrix transfer technique is also used, but the parabolic potential in each cell is approached by a constant. This indicates that his method would apply to either low magnetic fields or high periodic potentials. These requirements are not always satisfied in periodic layered structures produced by molecular beam epitaxy, where the Kronig-Penney model should precisely apply.

ACKNOWLEDGMENTS

Work performed in the framework of the joint project ESIS (Electronic Structure in Solids) of the University of Antwerp and the University of Liège. One of us (J.P.V.) would like to thank the Fonds National de la Recherche Scientifique, Belgium for financial support.

[1]See, for instance, J. G. Mavroides, in *Optical properties of Solids*, edited by F. Abelès, (North-Holland, Amsterdam, 1972), p. 351.
[2]*Electronic Properties of Quasi-Two-Dimensional Systems*, edited by J. J. Quinn and P. J. Stiles (North-Holland, Amsterdam, 1976), as reprinted from Surf. Sci. 58, 1 (1976).
[3]*Proceedings of Thirteenth International Conference on the Physics of Semiconductors, Rome 1976,* edited by F. G. Fumi (Tipografia Marves, Rome, 1976).
[4]J. P. Kotthaus, G. Abstreiter, and J. F. Koch, Solid State Commun. 15, 517 (1974).
[5]G. Abstreiter, P. Kneschourek, J. P. Kotthaus, and J. F. Koch, Phys. Rev. Lett. 32, 104 (1974).
[6]S. James Allen, Jr., D. C. Tsui, and J. V. Dalton, Phys. Rev. Lett. 32, 107 (1974).
[7]J. P. Kotthaus and H. Küelbeck, Surf. Sci. 58, 199 (1976).
[8]K. Suzuki and Y. Kawamoto, J. Phys. Soc. Jpn. 35, 1456 (1973).
[9]G. Abstreiter, J. P. Kotthaus, J. F. Koch, and G. Dorda, Phys. Rev. B 14, 2480 (1976).
[10]W. Beinvogl, A. Kamgar, and J. F. Koch, Phys. Rev. B 14, 4274 (1976).
[11]M. von Ortenberg and R. Silbermann, Surf. Sci. 58, 202 (1976).
[12]W. Brawne, J. Lebech, and K. Saermark (private communication).
[13]T. Ando, Phys. Rev. B 13, 3468 (1976); Phys. Soc. Jpn. 36, 959 (1974); 36, 1521 (1974); 37, 622 (1974); 37, 1233 (1974); 38, 989 (1975).
[14]J. P. Vigneron and M. Ausloos (unpublished).
[15]R. Dingle, in Ref. 3, pp. 965–974.
[16]M. Abramowitz and I. A. Stegun *Handbook of Mathematical Functions* (Dover, New York, 1964), p. 685.
[17]I. S. Gradshteyn and I. M. Ryzhik, *Table of Integrals, Series and Products*, 4th ed. (Academic, New York, 1965).
[18]L. Schiff, *Quantum Mechanics* (McGraw-Hill, New-York, 1968).
[19]P. L. Taylor, Phys. Rev. B 15, 3558 (1977).